Theoretical Notes
Note 170

SC-RR-72 0173

MODELS FOR ELECTROMAGNETIC PULSE PRODUCTION FROM UNDERGROUND NUCLEAR EXPLOSIONS, PART IV: MODELS FOR TWO NEVADA SOILS

Charles N. Vittitoe

Weapon Effects Research Department
Sandia Laboratories
Albuquerque, New Mexico
87115

May 1972

ABSTRACT

The frequency variation of the electrical parameters of a sample of Nevada tuff is modeled by a Debye relaxation model. Less success occurs for similar modeling of a dry granite sample. Data from R. L. Ewing are used to estimate the secondary electron mean lifetime in the dry granite sample as 2×10^{-10} sec with a mobility of 111 esu. Difficulties with similar estimates for tuff are mentioned, together with resulting uncertainty in calculated electromagnetic fields close to an underground nuclear explosion. Appendices show that the model obeys the Kramers-Kronig relation and contain discussion of an interpretation of large dielectric constants.

ACKNOWLEDGEMENTS

The author is indebted to H. B. Durham and G. A. Kinemond for gathering references which contained the data on the tuff and granite samples used here. Robert Ewing graciously furnished his preliminary data on gamma ray-induced conductivity in granite. Helpful discussions with S. L. Thompson and A. C. Switendick in addition to those mentioned above are also acknowledged. L. G. Lee contributed programming aid. F. Biggs and R. E. Lighthill provided excellent evaluation of coefficients to represent the frequency variation of the sample electrical properties.

TABLE OF CONTENTS

MODELS FOR ELECTROMAGNETIC PULSE PRODUCTION FROM UNDERGROUND NUCLEAR EXPLOSIONS, PART IV: MODELS FOR TWO NEVADA SOILS

INTRODUCTION

During typical underground nuclear bursts in Nevada, numerous instrumentation cables extend very close to the explosion center. Often these cables are embedded in concrete, soil, rock, or other filler materials. Near the burst a close-in electromagnetic pulse (EMP) will be produced in the surrounding materials. The EMP then scatters from the embedded conductors and induces currents which may interfere with the measurement of such quantities as weapon diagnostics or system hardness. In this report the two extremes of Nevada-type soil are treated in an attempt to bracket the variation of the parameters considered as the soil type changes. Samples of tuff and granite are modeled with Debye relaxation parameters to account for frequency-dependent properties. The Compton electron current provides the driving force for the EMP. Properties of the material determine how well the EMP couples energy into the cables and other nearby conductors. Radiation-induced conductivity is also discussed, since it must be included in the electric field calculation.

THE GROUND MODEL

In this section the soil is physically modeled in an attempt to account for the frequency-dependent electrical permittivity and conductivity. A model treated by Longmire and Longley[1] has the advantage of allowing a time domain solution for the current density in the soil after the applied electric field intensity is given. The Debye relaxation model treated next is shown to give the same frequency variation with additional freedom in the choice of sign for some of the parameters.

Following Longmire and Longley,[1] let us model the ground by the electrical circuit in Fig. 1. With an applied voltage of the form $V_o e^{i\omega t}$, the current I is given by

$$I(t) = \frac{V(t)}{R_o(t)} + i\omega C_\infty V(t) + \sum_n \frac{V(t)}{R_n + \frac{1}{i\omega C_n}} . \qquad (1)$$

Here, the R_i are allowed to vary with time to account for changes in the earth that might be produced by nuclear radiation. Changes in the capacitances are not expected to occur. Such capacitances are caused by cracks and holes in the soil. Under irradiation for short times, the dimensions are not expected to change. However, the electrical parameters of the lossy dielectric may vary. Radiation dose rates must be extremely large to change the number density for a particular type of molecule in the soil. Hence dielectric constant changes are not expected (see Appendix A). However, the soil conductivity will vary with radiation dose. In fact, the radiation

is likely to produce resistance in parallel with each of the capacitors and, hence, augment the shunt resistance caused by their lossy dielectrics which is accounted for by R_o. This latter shorting should depend upon the dielectric material which might be air or water.

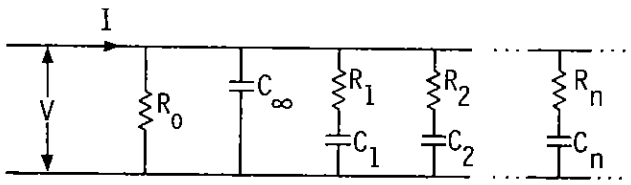

Fig. 1 Frequency-dependent electrical model of the ground (Longmire & Longley).

Let us assume that the voltage V in Fig. 1 is applied to a length L_1 of a cube of the soil by means of a parallel plate capacitor as indicated in Fig. 2. Division of Eq. (1) by L_1 then converts V(t) to E(t). If the area of the plates is A (or, equivalently, consider the volume of cross-sectional area A in a parallel plate capacitor of infinite area), division by A converts the current to a current density. Equation (1) can then be written as

$$j(t) = \frac{L_1}{R_o(t)A} E(t) + \frac{i\omega C_\infty L_1}{A} E(t) + \sum_n \frac{L_1}{R_n A + \frac{A}{i\omega C_n}} E(t) .$$

With the definitions

$$\xi_i = \frac{L_1}{R_i A} , \quad \eta_i = \frac{4\pi C_i L_1}{A} , \quad \beta_i = \frac{4\pi \xi_i}{\eta_i} ,$$

this becomes

$$j(t) = \xi_o E(t) + \frac{i\omega\eta_\infty}{4\pi} E(t) + \sum_n \frac{\xi_n \omega^2 + i\omega\beta_n \xi_n}{\beta_n^2 + \omega^2} E(t) . \qquad (2)$$

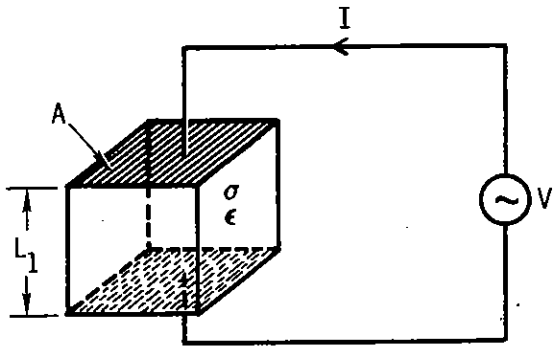

Fig. 2 Extension of the circuit model to a cube of lossy material inserted as a dielectric in a parallel plate capacitor.

Equation (2) may also be written

$$j(t) = \xi_o E(t) + \frac{i\omega\eta_\infty}{4\pi} E(t) + \sum_n a_n J_n(t) ,$$

where, for each frequency component ω in the applied voltage,

$$a_n J_{n\omega}(t) = \frac{E_\omega(t)}{\frac{1}{\xi_n} + \frac{4\pi}{i\omega\eta_n}} . \tag{3}$$

With $a_n = \xi_n$, Eq. (3) becomes

$$a_n J_{n\omega}(t) = \frac{i\omega a_n}{\beta_n + i\omega} E_\omega(t) . \tag{4}$$

Since each frequency component yields $\partial E_\omega / \partial t = i\omega E_\omega$, this becomes

$$a_n J_{n\omega} = \frac{a_n}{\beta_n^2 + \omega^2} \left[\beta_n \frac{\partial E_\omega}{\partial t} + \omega^2 E_\omega \right] . \tag{5}$$

Multiplication of (5) by β_n and addition of the time derivative of (5) yields

$$\left[a_n\beta_n + \frac{\partial a_n}{\partial t}\right] J_{n\omega} + a_n \frac{\partial J_{n\omega}}{\partial t} =$$

$$\left[a_n + \frac{a_n}{\beta_n^2 + \omega^2}\frac{\partial \beta_n}{\partial t} + \frac{\beta_n}{\beta_n^2 + \omega^2}\frac{\partial a_n}{\partial t} - \frac{2a_n\beta_n^2}{\left(\beta_n^2 + \omega^2\right)^2}\frac{\partial \beta_n}{\partial t}\right]\frac{\partial E_\omega}{\partial t}$$

$$+ \left[\frac{\omega^2}{\beta_n^2 + \omega^2}\frac{\partial a_n}{\partial t} - \frac{2a_n\beta_n\omega^2}{\left(\beta_n^2 + \omega^2\right)^2}\frac{\partial \beta_n}{\partial t}\right] E_\omega . \qquad (6)$$

When $\frac{\partial a_n}{\partial t} = \frac{\partial \beta_n}{\partial t} = 0$, the equation simplifies to

$$\beta_n J_{n\omega} + \frac{\partial J_{n\omega}}{\partial t} = \frac{\partial E_\omega}{\partial t} . \qquad (7)$$

Thus, outside the radiation region where resistances and capacitances are independent of time, the explicit frequency dependence drops out and summation over the frequencies in the applied electric field gives the time domain result obtained by Longmire and Longley:

$$\frac{\partial J_n}{\partial t} + \beta_n J_n = \frac{\partial E}{\partial t} . \qquad (8)$$

Since, for short irradiation times the capacitor dimensions, dielectric permittivities, and hence capacitances do not change,

$$\frac{\partial \beta_n}{\partial t} = \frac{\beta_n}{a_n}\frac{\partial a_n}{\partial t} .$$

The more general equation then simplifies to

$$\left[a_n\beta_n + \frac{\partial a_n}{\partial t}\right] J_{n\omega} + a_n \frac{\partial J_{n\omega}}{\partial t} =$$

$$\left[a_n + \frac{2\beta_n\omega^2}{\left(\beta_n^2 + \omega^2\right)^2}\frac{\partial a_n}{\partial t}\right]\frac{\partial E_\omega}{\partial t} + \left[\frac{\omega^4 - \beta_n^2\omega^2}{\left(\beta_n^2 + \omega^2\right)^2}\frac{\partial a_n}{\partial t}\right] E_\omega . \qquad (9)$$

One of Maxwell's equations yields:

$$\nabla \times \underline{H} = \frac{4\pi}{c} (\underline{J} + \sigma \underline{E}) + \frac{1}{c} \frac{\partial \underline{D}}{\partial t} . \tag{10}$$

If the curl of the magnetic field can be neglected, no driving current is present, and harmonic time dependence is assumed, then the total current is given by

$$\underline{j} = \left[\sigma + \frac{i\omega\epsilon}{4\pi}\right] \underline{E} . \tag{11}$$

A material is classified as a good conductor if the conduction current density (σE) in (11) is large compared to the displacement current density $\left(\frac{i\omega\epsilon}{4\pi} E\right)$. A poor conductor is one in which the displacement current dominates. For the soils treated here, the two terms are of comparable size over some portion of the frequency range of interest. Consider a sample of Nevada tuff from near the Diamond Mine site. With $f = 10^7$ Hz, $\sigma = 0.02$ mho/m ($= 1.8 \times 10^8$ sec^{-1}) and $\epsilon = 30$,

$$\frac{4\pi\sigma}{\omega\epsilon} = 1.2 .$$

Thus the tuff becomes a poor conductor for frequencies greater than 10^8 Hz and a good conductor for frequencies lower than 10^6 Hz. A better insulating ground material with $\epsilon \approx 10$ and $\sigma \approx 10^{-4}$ mho/m is a poor conductor for frequencies greater than 2×10^6 and a good conductor for $f < 2 \times 10^4$ Hz. Comparison of Eq. (11) with the real and imaginary parts of Eq. (2) produces the frequency variations

$$\sigma = \xi_o + \sum_{n=1}^{N} \frac{a_n \omega^2}{\beta_n^2 + \omega^2} , \tag{12}$$

$$\frac{\epsilon}{4\pi} = \frac{\eta_\infty}{4\pi} + \sum_{n=1}^{N} \frac{a_n \beta_n}{\beta_n^2 + \omega^2} . \tag{13}$$

Following the suggestion of Longmire and Longley,[1] let us assume that

$$\beta_n = 2\pi \times 10^{n+1} \text{ sec}^{-1} , \tag{14}$$

with

$$\sigma_o = \xi_o \tag{15}$$

and

$$\epsilon_\infty = \eta_\infty . \tag{16}$$

Forms similar to (12) and (13) with N = 1 were derived by Debye,[2] with a more concise method indicated by Jones.[3] Following Jones, let the electric field intensity and electric displacement be given by their Fourier transforms:

$$\underline{D}(t) = \int_{-\infty}^{\infty} \underline{\mathcal{D}}(\omega)\, e^{i\omega t}\, d\omega ,$$

$$\underline{E}(t) = \int_{-\infty}^{\infty} \underline{\mathcal{E}}(\omega)\, e^{i\omega t}\, d\omega .$$

Then

$$\underline{D}(t) = \int_{-\infty}^{\infty} \epsilon(\omega)\underline{\mathcal{E}}(\omega)\, e^{i\omega t}\, d\omega . \tag{17}$$

In general, ϵ is a complex function of frequency that is here assumed to approach a real, positive constant (ϵ_∞) as $|\omega| \to \infty$. Therefore,

$$\int_{-\infty}^{\infty} \epsilon(\omega)\, e^{i\omega t}\, d\omega = 2\pi \left[\epsilon_\infty \delta(t) + \alpha(t)\right] , \tag{18}$$

where

$$\alpha(t) = \frac{1}{2\pi} \int_{-\infty}^{\infty} \left[\epsilon(\omega) - \epsilon_\infty\right] e^{i\omega t}\, d\omega . \tag{19}$$

Substitution of the transform of $\underline{E}(t)$ into (17) and use of (18) gives

$$\underline{D}(t) = \epsilon_\infty \underline{E}(t) + \int_{-\infty}^{\infty} \underline{E}(t')\alpha(t - t')\, dt' . \tag{20}$$

In the special case when $\alpha = 0$, no dispersion occurs and the more usual dielectric constant is obtained. When it is assumed that at $t = 0$ a disturbing electric field intensity is applied, the relaxation processes associated with $\alpha(t)$ do not occur for $t < 0$. Hence, $\alpha(t < 0) = 0$. This changes the upper limit of integration in (20) to t. If we generalize the treatment by Jones[3] and assume the relaxation is caused by a series of distinct processes (such as damped motion of various types of free-charge, damped reorientation of polar molecules, and possible electrochemical processes), the $\alpha(t)$ can be represented by a series

$$\alpha(t) = \sum_{n=1}^{N} \alpha_n \exp(-t/\tau_n) \tag{21}$$

for $t > 0$. If the material has a conductivity at zero frequency, this can be represented by the separation of an $n = 0$ from the summation and the assumption that $\omega\tau_o = \infty$ for all ω. Then the complex dielectric constant includes the DC conduction term as well. In that case, the transform of (19) gives

$$\epsilon(\omega) - \epsilon_\infty = \sum_{n=1}^{N} \frac{\alpha_n \tau_n}{1 + i\omega\tau_n} - \frac{4\pi i \sigma_o}{\omega} . \tag{22}$$

Separation into real and imaginary parts gives

$$\epsilon_r(\omega) = \epsilon_\infty + \sum_{n=1}^{N} \frac{\alpha_n \tau_n}{1 + \omega^2 \tau_n^2} , \tag{23}$$

$$\epsilon_i(\omega) = -\sum_{n=1}^{N} \frac{\omega \alpha_n \tau_n^2}{1 + \omega^2 \tau_n^2} - \frac{4\pi\sigma_o}{\omega} , \tag{24}$$

where $\epsilon(\omega) = \epsilon_r(\omega) + i\epsilon_i(\omega)$. The imaginary part may also be written in a form in which the conductivity is better specified:

$$\epsilon_i(\omega) = -\frac{4\pi}{\omega}\left[\sigma_o + \sum_{n=1}^{N} \frac{1}{4\pi} \frac{\alpha_n \tau_n^2 \omega^2}{1 + \omega^2 \tau_n^2}\right] .$$

For the case $N = 1$ and $\sigma_o = 0$, Eqs. (23) and (24) are known as the Debye equations and have been found applicable to dilute solutions[3] and some earth materials.[4] (Appendix B indicates that the usual dispersion relation is satisfied by this form of the dielectric constant.)

The α_n represent the amplitude of physical relaxation processes and must be real. Since damping is expected, the τ_n are required to be real and positive. However, the α_n may be negative. Because of production of damping by inertial, interatomic, and intermolecular forces, some processes may occur which induce an electric polarization opposite to the applied electric field intensity. For example, a polarized molecule might interact with its neighbors to induce a polarization in the direction opposite to the applied field. Such a reaction might be more probable at low frequencies where reaction with neighbors could be more important.

Wait and Fuller[5] have used a form similar to Eqs. (23) and (24) in modeling the earth's dispersive quantities by Debye relaxation processes. Their equations have the forms (MKS units):

$$\frac{\epsilon(\omega)}{\epsilon_o} = \sum_{m=1}^{M} \left[\gamma_m + \frac{\delta_m - \gamma_m}{1 + (\omega\tau_m)^2}\right] ,$$

$$\sigma(\omega) = \sigma_o + \sum_{m=1}^{M} \frac{\omega^2 \epsilon_o \tau_m (\delta_m - \gamma_m)}{1 + (\omega\tau_m)^2} .$$

With the substitutions

$$\epsilon_\infty = \sum_{m=1}^{M} \gamma_m \epsilon_o ,$$

$$\beta_m = 1/\tau_m ,$$

$$a_m = \beta_m \epsilon_o (\delta_m - \gamma_m) ,$$

and conversion to a consistent set of units, the Wait-Fuller results are easily shown to be equivalent to those of Longmire and Longley in Eqs. (12) and (13).

The standard treatment for dispersion theory assumes that each charged particle of mass m_i interacts with a harmonic electromagnetic field. Various degrees of sophistication may include a restoring force $\left(-m\omega_i^2(\underline{x}_i - \underline{x}_{io})\right)$, a damping force $(-m_i d_i \dot{\underline{x}}_i)$ proportional to the particle velocity, the electric field contribution to the force $(q_i \underline{E}_{total})$, and perhaps magnetic forces on the particle in addition to the radiation reaction terms. Where the latter two forces are neglected, the displacement of the charge is

$$\underline{x}_i = \frac{q_i \underline{E}_{total}}{m_i\left(\omega_i^2 - \omega^2 + i\omega d_i\right)} .$$

Thus the induced polarization can be positive or negative, depending on the relative sizes of the various parameters. For an atom the natural frequencies $\omega_i/2\pi$ of the electrons range from visible to ultraviolet. For molecules there are additional terms because of the vibration of the nuclei about equilibrium positions and because of molecular rotations. These frequencies are in the infrared part of the spectrum.[3] Small crystals in a material may interact with an electromagnetic field, giving still smaller natural frequencies that would produce anomalous dispersion at radio frequencies.

In fitting experimental data to evaluate the parameters in Eqs. (12) and (13), the a_n might be restricted to positive values since they represent the inverse of a resistance per unit length. However, negative allowed values of α_n in Eqs. (23) and (24) indicate the a_n can indeed be negative. This might be treated in the circuit model as an interaction between neighboring capacitors.

MODEL FOR NEVADA TUFF

Data on a sample of Nevada tuff have been collected by the USGS, and by Grubb.[6] The dielectric constant variation with frequency is illustrated in Fig. 3. Part of these data is listed in Table I.

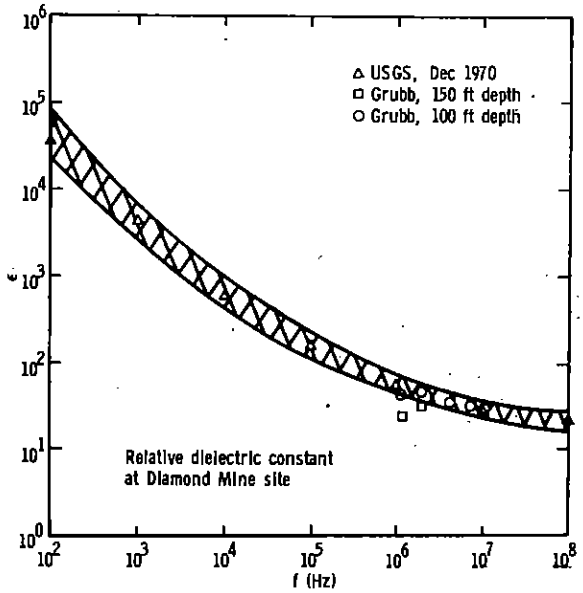

Fig. 3 Dielectric constant of tuff as a function of frequency. The crosshatched area indicates the variation with various core samples chosen.

TABLE I. Early USGS Electrical Parameters for Nevada Tuff Sample*

f(Hz)	ϵ	σ (mho/m)	σ (10^7 sec^{-1})
10^2	35100	0.0124	11.2
10^3	4110	0.0128	11.5
10^4	620	0.0131	11.8
10^5	166	0.0138	12.4
10^6	45	0.0158	14.2
10^7	25	0.0214	19.3
10^8	22	0.0555	50.0

*See Appendix C for additional comments concerning large permittivity values.

Data for these seven frequencies were substituted into (13) to obtain the seven coefficients ϵ_∞ and a_n for n = 1, ..., 6. Substitution back into (13) yields reasonable agreement with data in the range $2\pi \times 10^2 < \omega \leq 10^8$ sec^{-1}. Using these same coefficients in (12) with an estimate for σ_o gives less satisfactory agreement with Fig. 4. In view of the spread in data, the coefficients are still a reasonable representation of the tuff conductivity. Solving the problem in the reverse order is not nearly so satisfying. The variation of ϵ over about four orders of magnitude gives a better determination of the coefficients than the conductivity data which vary only within a factor of two over the ω range plotted.

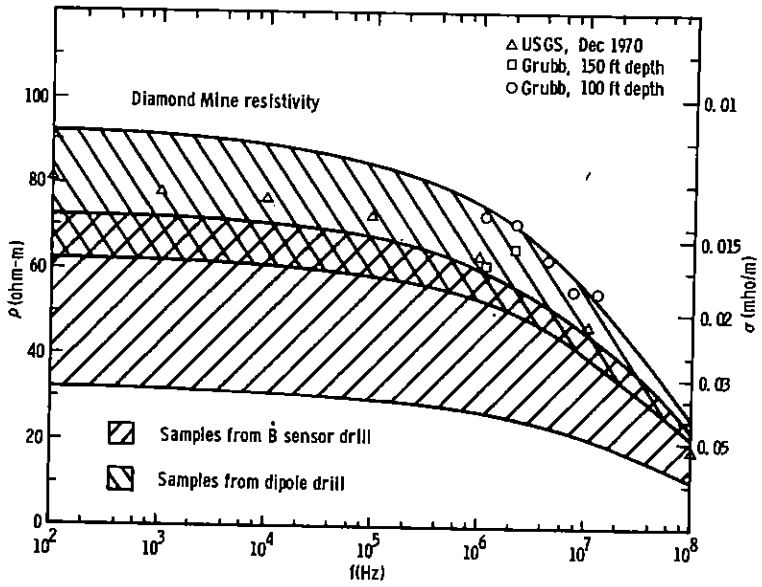

Fig. 4 Measured resistivity of tuff as a function of frequency. The cross-hatched areas indicate the variation with sample chosen.

A somewhat better fit is possible to the frequency variation of ϵ and σ if the β_n are also allowed to vary. A program has been developed by Biggs and Lighthill[7] which will use Eqs. (12) and (13) and find coefficients ϵ_∞, σ_o, β_n, and a_n. This minimizes the square of a normalized difference between a set of (ω, ϵ, σ) data points fed in and the calculated values of ϵ, σ. The fit may not be the absolute minimum to the fitting parameter but is at least a local minimum. The coefficients from this program are listed in Table II with the resulting curves illustrated in Figs. 5 and 6. These results are consistent with the data, indicating that Debye relaxation processes properly account for the frequency variation of the electrical properties of tuff within the frequency range of the data.

TABLE II. Coefficients for a Sample of Tuff

n	a_n	β_n	ϵ_∞	σ_o
1	3.02×10^6	7.74×10^2	9.72	1.13×10^8 sec^{-1}
2	2.88×10^6	8.25×10^3		or
3	3.90×10^6	8.68×10^4		0.0126 mho/m
4	1.28×10^7	1.07×10^6		
5	2.63×10^7	1.50×10^7		
6	8.14×10^8	7.07×10^8		

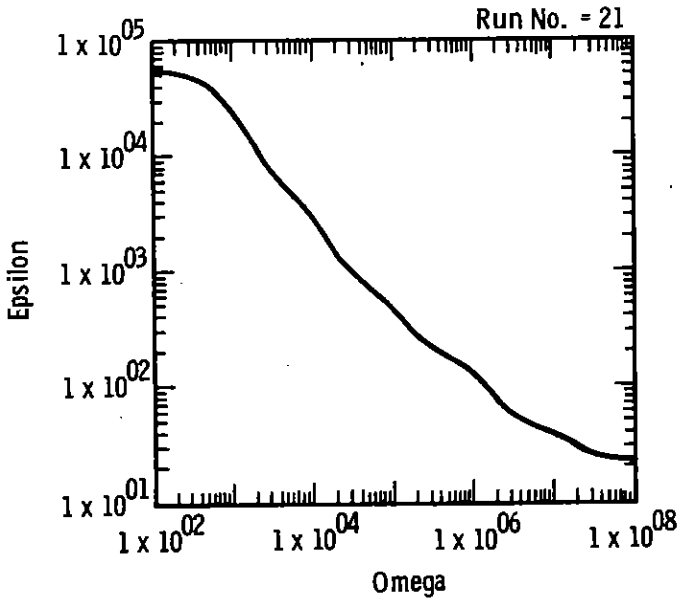

Fig. 5 Permittivity variation with angular frequency predicted by fit to data for Nevada tuff sample.

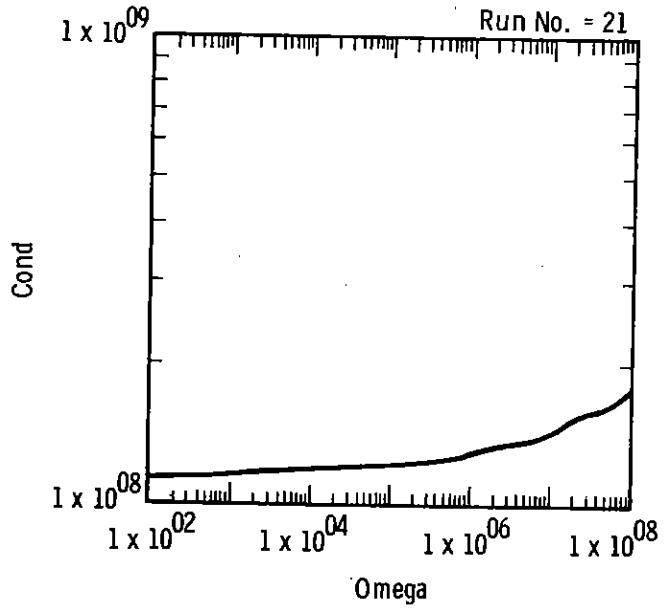

Fig. 6 Conductivity (sec^{-1}) of a sample of Nevada tuff as predicted by fit to σ, ϵ data.

MODEL FOR DRY GRANITE

As an example of a better insulating ground material, G. A. Kinemond of Sandia Laboratories has furnished some data on dry granite. The data are listed in Table III.

TABLE III. Electrical Parameters for Granite Sample

f(Hz)	ϵ	σ(mho/m)	$\sigma(sec^{-1})$
10^2	10.20	7.00×10^{-7}	6.30×10^3
10^3	9.95	2.21×10^{-6}	1.99×10^4
10^4	9.70	7.30×10^{-6}	6.57×10^4
10^5	9.46	2.40×10^{-5}	2.16×10^5
10^6	9.11	7.84×10^{-5}	7.06×10^5
10^7	8.71	2.62×10^{-4}	2.36×10^6
10^8	8.30	8.80×10^{-4}	7.92×10^6

Straightforward substitution into Eq. (12) yields values of a_n which produce oscillations in $\epsilon(\omega)$. The UNFOLD program[8] has the unique capability of least square fitting theoretical curves to data with added requirements such as constraining the function to be ≥ 0, or having bounds on higher derivatives in order to reduce oscillations. Accuracy of the data is one of the input variables which limit the variations forced by the added constraints. Substitution of the data into (13) with $\beta_n = 2\pi \times 10^{n+1}$, as before, yields the coefficients

$$\begin{aligned} \epsilon_\infty &= 8.39 , \\ a_1 &= 1.34 \times 10^1 , \\ a_2 &= 1.26 \times 10^2 , \\ a_3 &= 1.21 \times 10^3 , \\ a_4 &= 1.32 \times 10^4 , \\ a_5 &= 1.84 \times 10^5 , \\ a_6 &= 2.81 \times 10^6 . \end{aligned} \tag{25}$$

The agreement with ϵ data is excellent as indicated in Fig. 7. However, the conductivity predicted by Eq. (12) is too low. This might not be too serious a difficulty if the function $\frac{4\pi\sigma}{\omega\epsilon}$ for the granite sample were small over the limits of interest. Unfortunately, the data from Table II indicate that the function is small only at the upper end of the frequency scale, $f > 10$ MHz. Thus, underestimates of the conductivity can be tolerated only at high frequencies. In like manner, underestimates of ϵ appear to be tolerable for frequencies below 10^2 Hz, since the granite is a "good conductor" in that region.

Substitution of the data into the conductivity equation (12) produces coefficients which cause the ϵ to vary over nearly an order of magnitude, as seen in Fig. 8, and thus is a poorer fit to the data.

Figure 9 shows the results when the coefficients are estimated from the separate ϵ and σ results and after processing with the Biggs-Lighthill program[7] mentioned earlier, and indicates that these dry granite data do not fit the model treated here. For further calculations with this material, the coefficients in Eq. (25) are recommended if the signal propagation speed is to have the correct frequency variation. The coefficients in Fig. 9 are recommended if conductivity effects are to be emphasized.

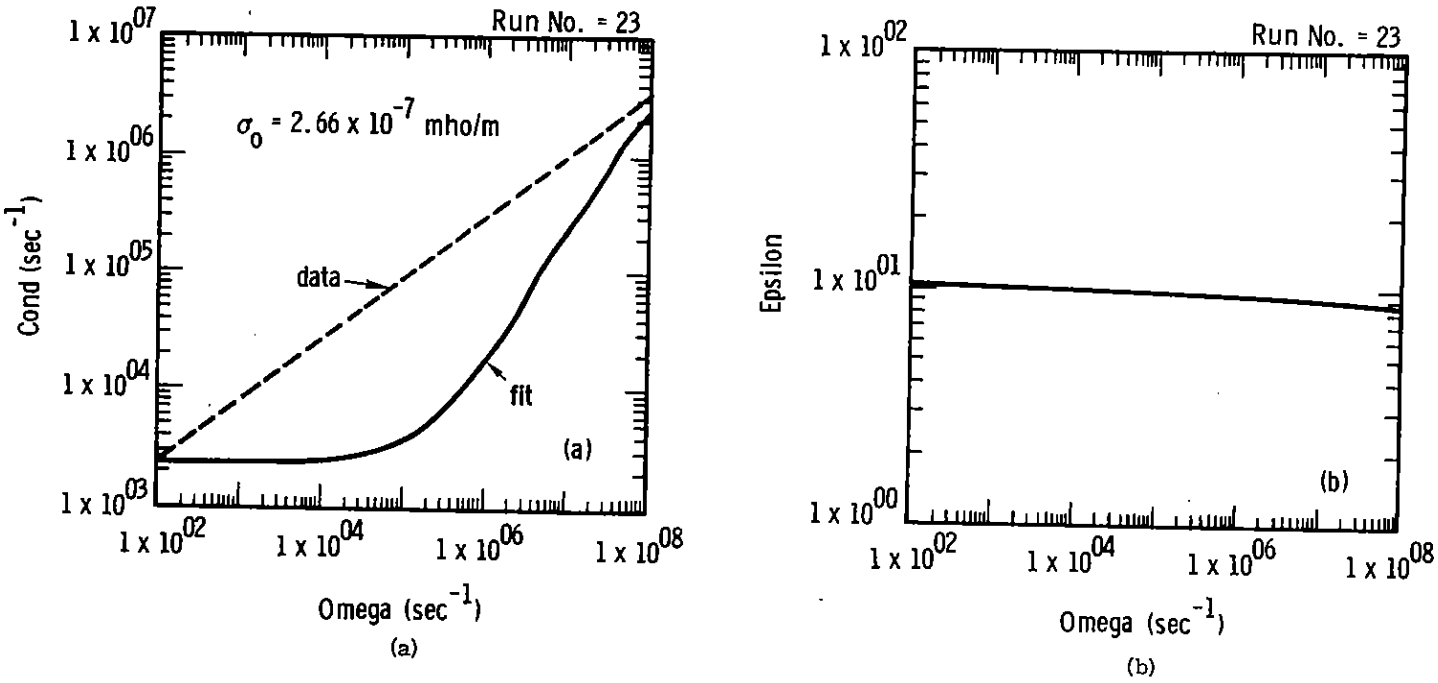

Fig. 7 The conductivity (sec^{-1}) and permittivity resulting from a fit to the granite permittivity data.

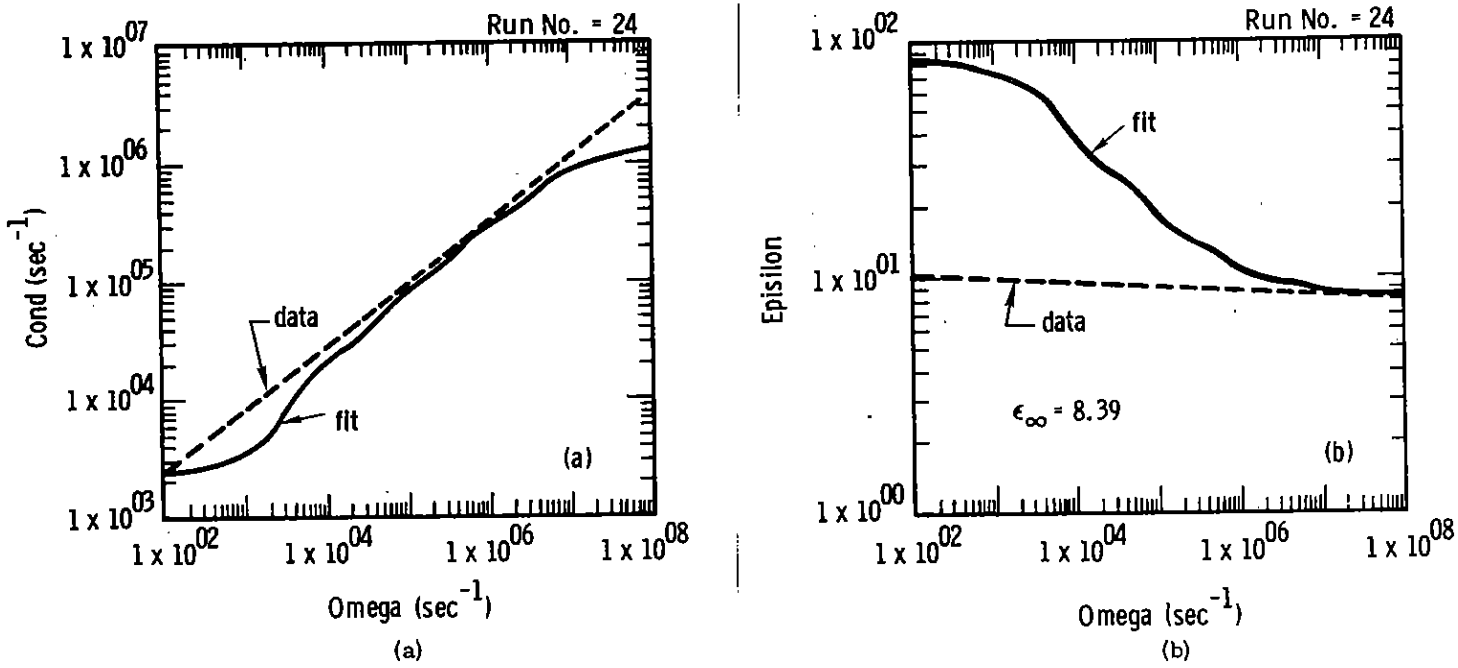

Fig. 8 The conductivity and permittivity resulting from a fit to the granite conductivity data.

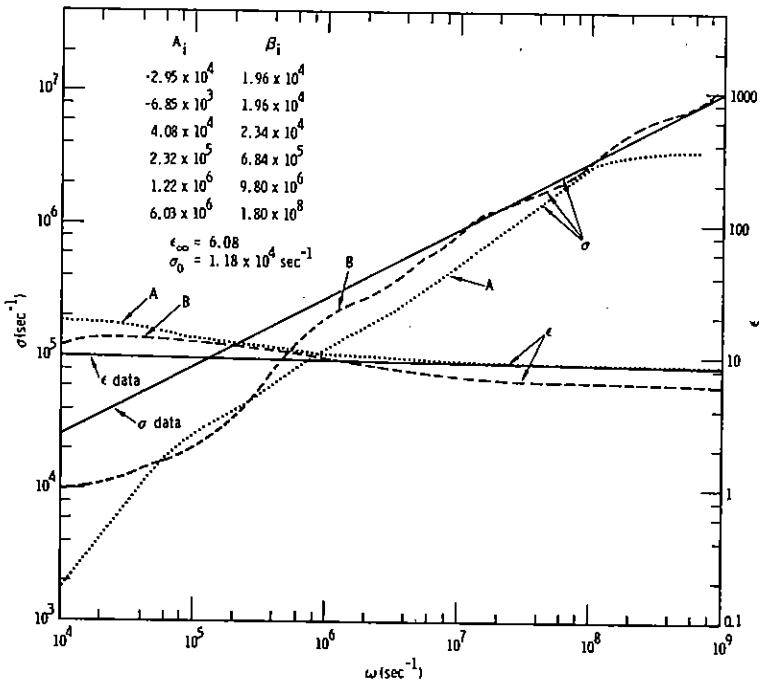

Fig. 9 The conductivity and dielectric constant for a dry granite sample. A indicates coefficients estimated from separate fits to ϵ and σ; B indicates coefficients after processing for better estimates of a_n and β_n.

CONDUCTIVITY ENHANCEMENT OF TUFF CAUSED BY GAMMA RADIATION

Solution of specific problems would be greatly simplified if Eq. (9) could be converted to the form of Eq. (8). For Nevada tuff, the a_n ($\sim 1/R_n$) were found to be on the order of 3×10^6 to 3×10^7 sec^{-1} except for n = 6, while $\sigma \approx 1.13 \times 10^8$ sec^{-1}. Hence R_o is the smallest resistance in the circuit and dominates the current flow except for frequencies $\gtrsim 10^8$ Hz where the n = 6 term is significant. In a typical nuclear radiation environment the Compton current density and induced voltages initially follow the $\dot{\gamma}$ pulse, with e folding times near 1 shake (10^{-8} second). The highest frequency contributing significantly to the source is then expected to be less than 10^8 Hz. Recall that

$$\frac{\partial a_n}{\partial t} = \frac{1}{R_n^2} \frac{\partial R_n}{\partial t} = a_n^2 \frac{\partial R_n}{\partial t} . \qquad (26)$$

With the assumption that the initial resistance R_n is large compared to any changes that occur in $\sim 10^{-8}$ second, neglect of the time variation of a_n is justified and Eq. (9) may be replaced by Eq. (8).

As the Compton electrons slow down, secondary electrons are created and the ground conductivity is enhanced. The conductivity of the ground is given by

$$\sigma = \sigma_{o1} + \sum_{i=1}^{N} \mu_i \eta_i q_i \,, \tag{27}$$

where σ_{o1} is the ambient value and the summation is for the N species of charge carriers formed by the radiation. Because of the relatively high σ_{o1} expected ($\sim$0.01 mho/m) and the larger mobility of electrons compared to ions, only electrons are included here, i.e., N = 1. The chemical composition of tuff is assumed to be SiO_2, 70 percent; H_2O, 10 percent; $A\ell_2O_3$, 12 percent; and K_2O, 8 percent. For crystalline SiO_2, Van Lint[9] suggests an increase in conductivity given by

$$\Delta\sigma = 4 \times 10^{-29}\, Q \text{ mho/m} \,, \tag{28}$$

where Q is the energy deposition rate in MeV m^{-3} sec^{-1}. In terms of the gamma-ray flux $\dot{\gamma}$ (MeV m^{-2} sec^{-1}),

$$Q = -\frac{d\dot{\gamma}}{dz} = \frac{\dot{\gamma}}{\lambda} \,, \tag{29}$$

$$\Delta\sigma(\text{mho/m}) = \frac{4 \times 10^{-29}}{\lambda(\text{m})}\, \dot{\gamma}\left(\frac{\text{MeV}}{\text{m}^2\ \text{sec}}\right) \,,$$

or

$$\Delta\sigma\ (\text{sec}^{-1}) = \frac{36 \times 10^{-14}}{\lambda(\text{cm})}\, \dot{\gamma}\left(\frac{\text{MeV}}{\text{cm}^2\ \text{sec}}\right) . \tag{30}$$

Data indicate that other materials have changes in conductivity varying as $\dot{\gamma}$ to some power.[10] The exponent, however, always appears to be close to one. Such a formula neglects the specific electron depletion processes that would be expected to introduce a time delay in the conductivity decay after the $\dot{\gamma}$ peak has occurred.

In the soil the secondary electron number density might be approximated by

$$\frac{dn_e}{dt} = S_e + \alpha_{o1} n_e + \beta_{o1} n_e^{\,2} \,, \tag{31}$$

where

$$\alpha_{o1} = -10^{9}\ \text{sec}^{-1},$$

$$\beta_{o1} = -10^{-7}\ \text{cm}^{3}/\text{sec},$$

$$S_e = \xi f_e,$$

$$\xi = \frac{\text{number of electrons produced by each primary electron}}{R},$$

$$\xi = \rho(1.23 \times 10^{5}\ \text{cm}^{2}/\text{gm}),$$

and 33 eV are assumed to produce each secondary electron. The Compton electron flux in the soil (f_e) can be approximated by

$$f_e = k f_\gamma, \tag{32}$$

where k is in the range 0.005 through 0.01. The proportionality constant is the ratio of the mean forward range of electrons to the Compton interaction mean free path of the gamma rays. This equation also assumes steady state conditions; i.e., the gamma flux does not change significantly in the time difference between a Compton electron and a gamma ray traveling the Compton electron's mean forward range. The mean forward range of the latter in air is approximated by

$$R = \frac{0.312T^{2}}{(0.30 + T)\rho}, \tag{33}$$

where ρ is the density (gm/cm^3), T is the electron kinetic energy in MeV, and R is the electron range in centimeters.[11] Extension of this to Nevada tuff with $\rho = 1.91\ \text{gm/cm}^3$ and T = 1 MeV gives R = 0.126 cm. An electron speed of 0.9c indicates that 4×10^{-12} second is required to travel R. Thus the quasi-static approximation is reasonable for the Compton electron flux.

The parameter β_{o1} is an order of magnitude estimate obtained from Bates.[12] In sea level air α_{o1} would be $-10^{+8}\ \text{sec}^{-1}$, mainly because of three-body attachment to O_2 molecules. In the tuff the α_{o1} might be assumed to attach more quickly because of the higher density. It might also be argued that the value should be lower because of the lack of proper molecules for attachment. Data for parameters α_{o1} and β_{o1} are necessary to improve the electron number density determination.

If $dn_e/dt \ll \xi f_e$, the steady-state approximation is reasonable and (31) may be solved for n_e. In the solution of the resulting quadratic equation, the ambiguity concerning the two solutions is resolved by requiring n_e to be positive.

If the β_{o1} term can be neglected (consistent with the data for SiO_2) and dn_e/dt can be neglected, a form equivalent to van Lint's is obtained:

$$\Delta\sigma = \mu e n_e = -\mu e \frac{\xi k f}{\alpha_{o1}} \gamma \quad . \tag{34}$$

Thus in this approximation, equating to van Lint's expression gives a result for crystalline SiO_2:

$$\frac{\mu(\text{esu})}{\left|\alpha_{o1}\ (\text{sec}^{-1})\right|} \approx 1.8 \times 10^{-8} \quad . \tag{35}$$

In the next section it can be observed that this relation applies reasonably well to granite; a following paragraph indicates that it may apply to tuff also. The large SiO_2 content in these materials may account for this behavior.

An estimate of the electron mobility is now required. Modeling of the tuff as condensed air and neglecting possible electric field variation give the electron mobility

$$\mu = 10^6 \text{ esu } \rho_{air}/\rho_{tuff} \quad , \tag{36}$$

where

$$3 \times 10^6 \text{ esu of mobility} = 1 \text{ m}^2 \text{ V}^{-1} \text{ sec}^{-1} . \tag{37}$$

Such a formulation oversimplifies the problem and is only justified by the lack of data for a better estimate.

An additional difficulty occurs because of the pressures which may be present. For example, a gamma flux of 2×10^{11} r/sec incident upon an SiO_2 sample will deposit about 4.8 cal per gm of material for a pulse width of 10^{-8} sec. Assumption of a density near 2 gm/cc and a Grüneisen coefficient near one results in a pressure increase of 0.4 atmosphere. At larger flux rates near a weapon cavity in Nevada, proportionally larger pressure increases are expected simply because of the deposition of gamma-ray energy.[13] Shock waves typically travel at around 20 cm/μsec. Hence these pressure increases arrive much later in time. Such pressure effects are expected to change the electron mobility and attachment parameters.

Equation (36) gives $\mu \approx 644$ esu for the assumed tuff. Back substitution into (35) gives an estimate for α_{o1}:

$$-\alpha_{o1} \text{ (est)} = 3.6 \times 10^{10} \text{ sec}^{-1} \quad .$$

This attachment rate is somewhat larger than expected, and may not be reasonable for Nevada tuff. However, secondary electrons live about 10^{-12} second in water[14] and the tuff sample is estimated to be 10-percent H_2O. Thus the above estimate is conceivable.

CONDUCTIVITY ENHANCEMENT OF GRANITE CAUSED BY GAMMA RADIATION

Preliminary results are available for an experimental measurement of the conductivity of a dry granite sample subjected to the photon beam from the Hermes II accelerator.[15] At a flux of 2×10^{11} γ MeV/(cm^2 sec) the measured value was 1.045×10^{-3} mho/m±20 percent. The conductivity pulse had a full width at half-maximum of less than 5 nsec wider than the $\dot{\gamma}$ pulse. Field intensities up to 6×10^5 V/m were applied without producing breakdown as the pulse traversed the material. The van Lint expression for pure SiO_2 would predict a peak conductivity of 1.01×10^{-3} mho/m in this situation, in excellent agreement!

An analytical estimate of the Hermes gamma pulse shape is given in Fig. 10. Use of the parameters $-\alpha_{o1} = 5 \times 10^9$ sec^{-1} and $-\beta_{o1} \leq 3 \times 10^{-6}$ cm^3/sec results in the secondary electron density in Fig. 11. Since the n_e only rises to 1.76×10^{14} electrons/cm^3, the α_{o1} term dominates the secondary electron attachment in the differential equation. For comparison, $-\alpha_{o1}$ values of 10^9 sec^{-1} and 10^{10} sec^{-1} have results as indicated. Experiments at larger dose rates are required to better define β_{o1} for granite. Thus the shape of the conductivity pulse is an aid to determination of the electron attachment parameters. The magnitude of the conductivity can also be used to estimate the mobility of the conduction electrons in the dry granite. Where it is assumed that the conductivity is attributable entirely to the electrons,

$$\Delta\sigma = \mu e n_e = 1.045 \times 10^{-3} \text{ mho/m} = 9.4 \times 10^6 \text{ sec}^{-1} . \qquad (38)$$

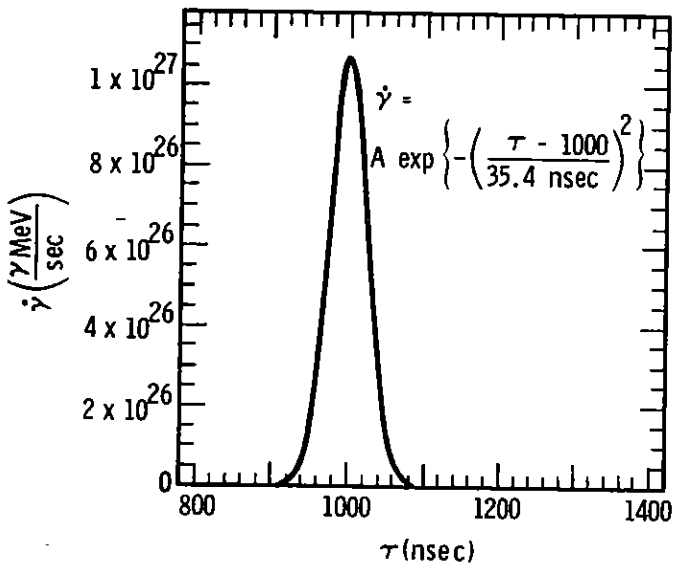

Fig. 10 Equivalent point source of gamma rays for Hermes pulse.

Equation (31) gives us the estimate for n_e illustrated in Fig. 11, i.e., a peak value of 1.76×10^{14} cm^{-3}. The estimate for electron mobility in granite is, from Eq. (38),

$$\mu = 111 \text{ esu} = 3.7 \times 10^{-5} \text{ m}^2 \text{ V}^{-1} \text{ sec}^{-1} .$$

The μ and α_{o1} are reasonably consistent with the earlier prediction in (35). Equation (36) would give a value of 490 esu for granite ($\rho = 2.5$ gm/cm^3), suggesting that the model of granite as condensed air leaves something to be desired.

Since the water displaces any air in the granite, addition of water would be expected to increase the absolute value of α_{o1} and decrease the electron mobility.

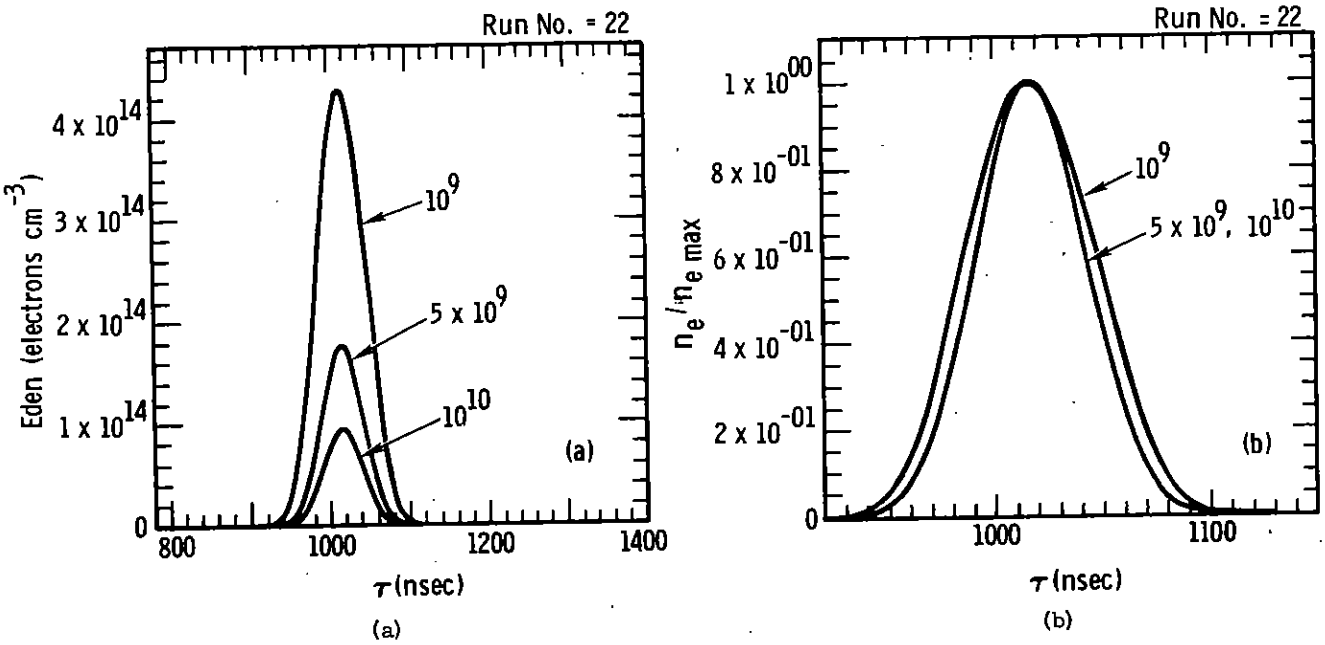

Fig. 11 (a) The electron density variation with time for three electron attachment parameters α_{o1} (sec^{-1}) and (b) normalized to unit amplitude.

DIFFICULTIES WITH TUFF PARAMETERS

Experimental conductivity data as a function of dose rate for tuff appear much more difficult to obtain. Typical grain size indicates that the sample should be 1/4-inch or more thick. The machined surfaces are somewhat rough, making electrical contact more difficult without trapping air. Presence of about 10 percent of water by weight and possibilities of air pockets in the tuff make extrapolation of results from other materials less dependable.

Let us consider briefly what limits can be placed upon the tuff parameters. Under the assumption that tuff is composed of molecules like those in granite, with a little more space for air or water, and that the electrons disappear by interactions with the molecules, the presence of air suggests a lower bound of 10^8 sec^{-1} for $-\alpha_{o1}$. A high concentration of water would increase this to values larger than 5×10^9 sec^{-1}. The shape of the conductivity pulse is reasonably invariant for $-\alpha_{o1} \geq 10^9$ sec^{-1}; thus 10^9 sec^{-1} appears reasonable. The electron mobility would increase sharply in air and decrease in water pockets. Hence, effective mobility might either increase or decrease from the granite value. Matching the induced conductivity also depends upon the α_{o1} value chosen.

In order to predict successfully the electromagnetic fields close to an underground nuclear explosion and the associated coupling of that electromagnetic energy into instrumentation cables that may be buried in the Nevada tuff, more information is required concerning the surrounding material properties. Conductivity measurements as a function of gamma-ray dose rate would allow the electron attachment parameters and mobility to be determined. With order-of-magnitude uncertainty in these parameters, a correspondingly high uncertainty must be expected in the calculated signals.

APPENDIX A

Effect of Gamma Radiation on Dielectric Constant

APPENDIX A

Effect of Gamma Radiation on Dielectric Constant

Definitions:

$\epsilon = 1 + 4\pi\chi_e$

χ_e = Electric susceptibility

$N_i \equiv$ Number of molecules of type i per unit volume

$\vec{p}_i \equiv$ Average dipole moment of each molecule of type i

$\eta_i \equiv$ Number of charge carriers of type i per unit volume

$\mu_i \equiv$ Mobility of charge carriers of type i

$\sigma = \sum_i q_i \mu_i \eta_i$

The dipole moment per unit volume is given by

$$\underline{P} = \chi_e \underline{E} = \sum_i N_i \vec{p}_i \ .$$

Thus, in the case of a scalar permittivity,

$$\epsilon = 1 + \frac{4\pi}{|\underline{E}|} \left| \sum_i N_i \vec{p}_i \right| .$$

For the dielectric constant to change significantly, the N_i must change. Large radiation doses are required for even one in 10^6 of the molecules of a certain type to be affected. Hence dielectric constant changes are not expected. The ionization does create new species such as secondary electrons with zero dipole moment and many types of ions. Relatively high mobility of the electrons causes conductivity to be affected easily by the radiation environment.

APPENDIX B

The Dispersion Relation

APPENDIX B

The Dispersion Relation

The Debye relaxation model of the electrical properties of the ground led to the complex dielectric constant

$$\epsilon(\omega) = \epsilon_\infty + \sum_{n=1}^{N} \frac{\alpha_n \tau_n}{1 + \omega^2 \tau_n^2} - \frac{4\pi i}{\omega} \left[\sigma_o + \sum_{n=1}^{N} \frac{1}{4\pi} \frac{\alpha_n \tau_n^2 \omega^2}{1 + \omega^2 \tau_n^2} \right] \tag{B.1}$$

given in Eqs. (23) and (24). Landau and Lifshitz[16] have shown that, as a result of causality, the real and imaginary parts are required to obey the Kramers and Kronig (or dispersion) relation. Following Landau and Lifshitz (with only the change in time dependence from $e^{-i\omega t}$ to $e^{i\omega t}$), the dispersion relations are

$$\epsilon_i(\omega) = -\frac{1}{\pi} P \int_{-\infty}^{\infty} \frac{\epsilon_r(x) - \epsilon_\infty}{x + \omega} \, dx - \frac{4\pi\sigma_o}{\omega} , \tag{B.2}$$

$$\epsilon_r(\omega) - \epsilon_\infty = -\frac{1}{\pi} P \int_{-\infty}^{\infty} \frac{\epsilon_i(x)}{x + \omega} \, dx . \tag{B.3}$$

Here, ϵ_∞ is the real limit of ϵ as $\omega \to \infty$, σ_o is the limit of the material conductivity as $\omega \to 0$, and P indicates the Cauchy principal value of the integral.

Landau and Lifshitz define $\epsilon(\omega)$ by the equation

$$\epsilon(\omega) = 1 + \int_0^{\infty} f(\tau) \, e^{i\omega\tau} \, d\tau . \tag{B.4}$$

Such a definition immediately yields

$$\epsilon(-\omega) = \epsilon^*(\omega) , \tag{B.5}$$

or that the real (imaginary) part of ϵ is an even (odd) function of ω. Such an approach omits the physical basis for this limitation. The term ϵ_i must be an odd function of ω to insure decay of an electromagnetic wave when its direction is reversed by the transformation $\omega \to -\omega$. The real part of the displacement vector $\underline{D}$ should also bear the same relation to the real part of $\epsilon\underline{E}$ when this transformation occurs. This is insured by ϵ_r being an even function of ω. The Debye relaxation model is easily seen to satisfy these criteria.

Direct substitution from (B. 1) into (B. 2), (B. 3) yields

$$-\frac{1}{\pi} P\int_{-\infty}^{\infty} \frac{\epsilon_r - \epsilon_\infty}{x + \omega}\, dx = -\sum_{n=1}^{N} \frac{\alpha_n \omega \tau_n^2}{1 + \omega^2 \tau_n^2}$$

and

$$-\frac{1}{\pi} P\int_{-\infty}^{\infty} \frac{\epsilon_i(x)}{x + \omega}\, dx = \sum_{n=1}^{N} \frac{\alpha_n \tau_n}{1 + \omega^2 \tau_n^2} ,$$

with proper treatment of the poles at $x = -\omega$ and $x = \pm i/\tau_n$. Helpful identities in the analysis include

$$P\int_{-\infty}^{\infty} \frac{1}{x + \omega}\, dx = 2\omega\, P\int_0^{\infty} \frac{dx}{x^2 - \omega^2} = 0$$

and

$$P\int_{-\infty}^{\infty} \frac{1}{x(x + \omega)}\, dx = 2P\int_0^{\infty} \frac{dx}{x^2 - \omega^2} = 0 .$$

Hence the Debye relaxation model of the electrical properties of the ground gives a complex dielectric constant that is consistent with the Kramers-Kronig relation.

APPENDIX C

Large Dielectric Constants

APPENDIX C

Large Dielectric Constants

Experimental values of dielectric constant sometimes attain values of 10^4 or 10^5. Such large values may be caused by layering of the material being measured. As an example, consider a parallel plate condenser composed of two parallel layers of material. One layer is assumed to have permittivity ϵ_1, zero conductivity, and thickness d. The other layer has negligible $\epsilon(\epsilon = 0)$, conductivity σ_2, and thickness qd. Simple analysis indicates that such a condenser behaves as if the space between the condenser plates were filled with a homogeneous dielectric having the complex dielectric constant

$$\epsilon = \frac{\epsilon_1(1 + q)}{1 + i\omega\epsilon_1 q/4\pi\sigma_2} .$$

This effect was reported in 1914 and is referred to as the Maxwell-Wagner mechanism in Kittel's work.[17] The equation suggests that this effect could be interpreted as one of the Debye relaxation mechanisms in Eq. (22). Kittel indicates that large permittivities may imply a thin dielectric layer (large q) and are only associated with materials that have large conductivities (σ_2). Such an effect can cause significant difficulty in the attachment of electrodes to a sample of Nevada tuff for parameter measurements. Such layering may also be present in the material itself.

As an example of the effect of this mechanism, consider the following parameters which may be appropriate for a measurement of Nevada tuff:

$$\sigma_2 = 0.0126 \text{ mho/m} = 1.13 \times 10^8 \text{ sec}^{-1} ,$$

$$q \gg 1 .$$

For $\epsilon_1 q = 10^3$, the real part of ϵ rises four orders of magnitude as the angular frequency decreases from 10^7 to 10^2 sec^{-1}. This variation is shown in the following illustrations for two choices of σ_2, Figs. C-1 and C-2.

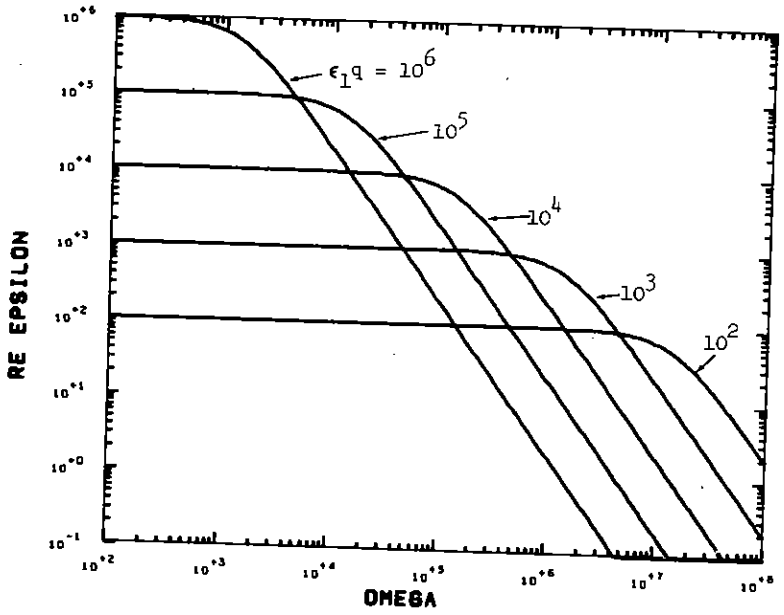

Fig. C-1 Illustration of the Maxwell-Wagner effect for various choices of $\epsilon_1 q$, $\sigma_2 = 1.13 \times 10^8$ sec^{-1}, and $q \gg 1$.

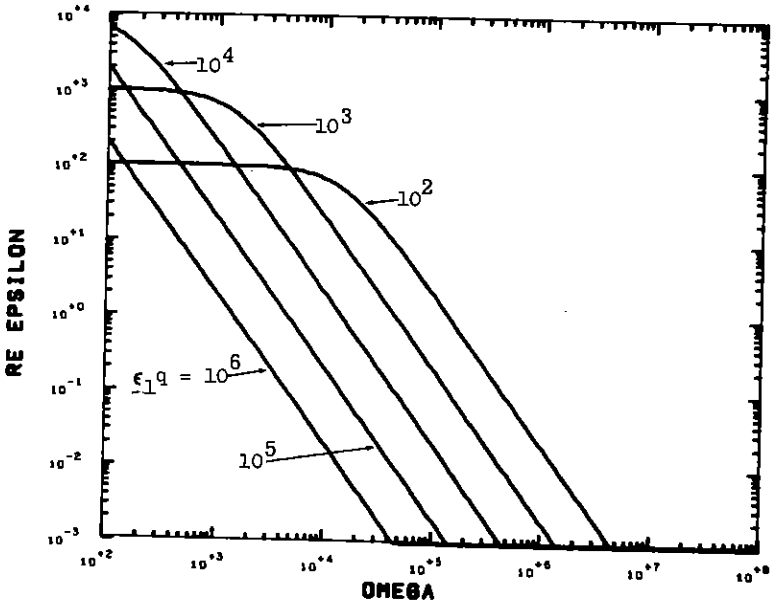

Fig. C-2 Illustration of the Maxwell-Wagner effect for various choices of $\epsilon_1 q$, $\sigma_2 = 1.13 \times 10^5$ sec^{-1}, and $q \gg 1$.

REFERENCES

1. C. L. Longmire and H. J. Longley, Time Domain Treatment of Media with Frequency-Dependent Electrical Parameters, Report MRC-N-1, Mission Research Corporation, P. O. Box 1356, Santa Barbara, California, 93101, March 12, 1971.

2. The Collected Papers of Peter J. W. Debye, Interscience Publishers, Inc., New York, 1954.

3. D. S. Jones, The Theory of Electromagnetism, The MacMillan Co., New York, 1964.

4. A. D. Petronsky, B. F. Vorisov, M. A. Kleymenov, and Yu. N. Troshkin, "Absorption Coefficients and Effective Electric Resistivities of Rock Blocks in Mining Areas," Akademiia Nauk SSSR, Izvestya, Physics of the Solid Earth, 10, 639 (1970).

5. J. A. Fuller and J. R. Wait, Electromagnetic Pulse Transmission in Homogeneous Dispersive Rock, Institute for Telecommunication Sciences, Department of Commerce, Boulder, Colorado, internal report, distributed at the Prime Argus EMP meeting, December 8-9, 1971, Sandia Laboratories, Albuquerque, New Mexico.

6. Table I data were obtained from the United States Geological Survey by private communication with Gary Kinemond, Sandia Laboratories, December 30, 1970. The Grubb data were taken by methods similar to those reported by R. N. Grubb and J. R. Wait, "In Situ Measurements of the Complex Propagation Constant in Rocks for Frequencies from 1 MHz to 10 MHz," Electronics Letters 7, 506 (1971).

7. Frank Biggs, Sandia Laboratories, private communication, February 1972.

8. F. Biggs and D. E. Amos, Numerical Solutions of Integral Equations and Curve Fitting, SC-RR-71 0212, Sandia Laboratories, September 1971.

9. V. A. J. van Lint, private communication to W. R. Graham of Rand Corporation, noted in January 1970.

10. W. H. Sullivan and R. L. Ewing, A Method for the Routine Measurement of Dielectric Photoconductivity, SC-DC-71 3696, Sandia Laboratories, July 1971.

11. H. J. Longley, Compton Current in the Presence of Fields for LEMP 1, LA-4348, Los Alamos Scientific Laboratory, April 1970.

12. D. R. Bates, Atomic and Molecular Processes, Academic Press, New York, 1962.

13. Pressure effects of gamma-ray energy deposition were suggested by J. Fleck at the Prime Argus EMP Meeting, December 8-9, 1971, Sandia Laboratories, Albuquerque, New Mexico.

14. Max S. Matheson, The Formation and Detection of Intermediates in Water Radiolysis, Radiation Research, Supplement No. 4; 1964, pp. 1-12; L. M. Dorfman and M. S. Matheson, "Pulse Radiolysis," Progress in Reaction Kinetics, Vol. 3, Pergamon Press, New York, 1965, pp. 237-301.

15. R. Ewing, Sandia Laboratories, private communication, December 1971.

16. L. D. Landau and E. M. Lifshitz, Electrodynamics of Continuous Media, Addison-Wesley Publishing Company, Inc., Reading, Massachusetts, 1960.

17. C. Kittel, Introduction to Solid State Physics, John Wiley & Sons, Inc., New York, 1959.